Ragged Synchronizability and Clustering in a Network of Coupled Oscillators

Przemyslaw Perlikowski, Andrzej Stefanski
and Tomasz Kapitaniak
Division of Dynamics, Technical University of Lodz,
Stefanowskiego 1/15, 90-924 Lodz, Poland
Email: przemyslaw.perlikowski@p.lodz.pl

Abstract— We show the phenomenon of complete synchronization in an network of coupled oscillators. We confirm that non-diagonal coupling can lead to the appearance or disappearance of synchronous windows (ragged synchronizability phenomenon) in the coupling parameter space. We also show the appearance of clusters (synchronization in one or more group) between coupled systems. Our numerical studies are confirmed by an electronic experiment.

I. INTRODUCTION

Over the last decade, chaotic synchronization in the networks of coupled dynamical systems has been intensively investigated, e.g.,[1-4]. An issue, the most often appearing during the study of any synchronization problem, is to determine a synchronization threshold, i.e. the strength of coupling which is required for the appearance of synchronization. In the case of identical systems (the same set of ODEs and values of the system parameters) a complete synchronization [3] can be obtained. The first analytical condition for the complete synchronization of regular sets (all-to-all or nearest-neighbour types of coupling) of completely diagonally coupled identical dynamical systems has been formulated in [5-7]. A complete diagonal (CD) coupling is realized by all diagonal components of output function (see Eq. (2)) for each pair of subsystems. Such a type of coupling induces a situation, when the condition of synchronization is determined only by the largest Lyapunov exponent of a node system and the coupling coefficient [5-9]. This property of CD coupling causes, that a synchronous range of a coupling parameter for time-continuous subsystems is only bottom-limited (Fig.1a) by a value of coupling coefficient being a linear function of the largest Lyapunov exponent [8]. If the coupling is partly diagonal (PD, i.e. realized by not all diagonal components of output function - see Eq. (3)) or non-diagonal (ND - also or only non-diagonal components of output function are used in the coupling - see Eqs (4) and (5)), then more advanced techniques like a concept called Master Stability Function (Sec. II) have to be applied [10]. This approach allows to solve the networks synchronization problem for any set of coupling weights, connections or number of coupled oscillators. Generally, in the literature dealing with PD or ND coupling problems dominate the works, where the synchronization ranges of a coupling parameter are only bottom-limited (like in the case of CD coupling - see Fig.1b) or they are ouble-limited (Fig.1c), i.e. there exists one window of synchronization (interval) in desynchronous regime [5-15]. In the previous work [16], we presented an example of ND coupled oscillators array, in which more than one separated ranges of synchronization occur when the coupling strength increases. We observe the appearance or disappearance of desynchronous windows in coupling parameter space, when the number of oscillators in the array or topology of connections changes. This phenomenon has been called the ragged synchronizability (RSA). This work describes the RSA phenomenon in an array of coupled van der Pol's oscillators. Our numerical studies are supported by a simple electronic experiment.

II. SYNCHRONIZABILITY OF COUPLED OSCILLATORS

In order to estimate the synchronization thresholds of a coupling parameter, we apply the idea

of the MSF [10]. Under this approach, the synchronizability of a network of oscillators can be quantified by the eigenvalue spectrum of the connectivity matrix, i.e. the Laplacian matrix representing the topology of connections between the network nodes. The dynamics of any network of N identical oscillators can be described in block form:

$$\dot{\mathbf{x}} = \mathbf{F}(\mathbf{x}) + (\sigma \mathbf{G} \otimes \mathbf{H}) \mathbf{x} \qquad (1)$$

where $\mathbf{x} = (\mathbf{x_1}, \mathbf{x_2}, \ldots, \mathbf{x_N}) \in \mathbf{R}^m$, $\mathbf{F}(\mathbf{x}) = (\mathbf{f}(\mathbf{x_1}), , \mathbf{f}(\mathbf{x_N}))$, $\mathbf{G}$ is the connectivity matrix (e.g. Eq. (13)), σ is the overall coupling coefficient, $\otimes$ is a direct (Kronecker) product of two matrices and $\mathbf{H} : \mathbf{R}^m \rightarrow \mathbf{R}^m$ is an output function of each oscillator's variables that is used in the coupling (it is the same for all nodes). Taking under consideration the classification of couplings mentioned in Sec. I we can present the following instances of output function for 3-D node system:

$$\mathbf{H} = \begin{bmatrix} 1 & 0 & 0 \\ 0 & 1 & 0 \\ 0 & 0 & 1 \end{bmatrix}, \qquad (2)$$

$$\mathbf{H} = \begin{bmatrix} 1 & 0 & 0 \\ 0 & 1 & 0 \\ 0 & 0 & 0 \end{bmatrix}, \qquad (3)$$

$$\mathbf{H} = \begin{bmatrix} 1 & 0 & 0 \\ 1 & 0 & 0 \\ 0 & 0 & 1 \end{bmatrix}, \qquad (4)$$

$$\mathbf{H} = \begin{bmatrix} 0 & 0 & 0 \\ 1 & 0 & 0 \\ 0 & 0 & 1 \end{bmatrix}. \qquad (5)$$

The $\mathbf{H}$ matrices exemplify CD (Eq. (2)), PD (Eq. (3)) and ND (Eqs (4) and (5)) coupling respectively. Eq. (5) defines the exemplary case of pure ND coupling, because all the diagonal components are equal to zero. In accordance with the MSF concept, a tendency to synchronization of the network is a function of the eigenvalues γ_k of connectivity matrix $\mathbf{G}$, $k = 0, 1, 2, \ldots, N - 1$. After block diagonalization of the variational equation of Eq. (1) there appear $N - 1$ separated blocks $\dot{\gamma}_k = [Df + \sigma\gamma_k D\mathbf{H}]$, (for $k = 0$, $\gamma_0 = 0$ is corresponding to the longitudinal mode), where γ_k represents different transverse modes of perturbation from synchronous state [10-13]. Substituting $\sigma\gamma = \alpha + i\beta$, where

$\alpha = Re(\gamma)$, $\beta = Im(\gamma)$ and γ represents an arbitrary value of γ_k, we obtain generic variational equation

$$\dot{\zeta} = [D\mathbf{f} + (\alpha + i\beta)D\mathbf{H}] \zeta, \qquad (6)$$

where ζ symbolizes an arbitrary transverse mode. The connectivity matrix $\mathbf{G} = \{G_{ij}\}$ satisfies $\sum_{j=1}^{N} G_{ij} = 0$ (zero row sum) so the synchronization manifold $\mathbf{x_1} = \mathbf{x_2} = \cdots = \mathbf{x_N}$ is invariant and all the real parts of eigenvalues γ_k associated with transversal modes are negative ($Re(\gamma_{k \neq 0} < 0)$. Hence, we obtain the following spectrum of the eigenvalues of $\mathbf{G}$: $\gamma_0 = 0 \geq \gamma_1 \geq \cdots \geq \gamma_{N-1}$. Now, we can define the MSF as a surface representing the largest transversal Lyapunov exponent (TLE) λ_T , calculated for generic variational equation, over the complex numbers plane (α, β). If all the eigenmodes corresponding to eigenvalues $\sigma\gamma_k = \alpha_k + i\beta_k$ can be found in the ranges of negative TLE then the synchronous state is stable for the considered configuration of the couplings. If an interaction between each pair of nodes is mutual and symmetrical there exist only real eigenvalues of matrix $\mathbf{G}$ ($\beta_k = 0$). In such a case, which is called the real coupling [12-13], the matrix $\mathbf{G}$ is symmetrical (see Eq. (13)) and the MSF is reduced to a form of a curve representing the largest TLE in function of a real number α fulfilling the equation

$$\alpha = \sigma\gamma. \qquad (7)$$

In Figs 1a–c typical examples of the MSF for CD coupling (Fig. 1a) and for PD or ND coupling (Figs 1b,c) are shown.

If the real coupling is applied to a set of oscillators with the MSF providing a single range of negative TLE as it is shown in Figs 1a, 1b and 1c, then the synchronous interval of a coupling parameter σ is simply reflected from the synchronous α-interval according to Eq. (7). For the case of MSF with double-limited α-interval of negative TLE (Fig. 1c) two transverse eigenmodes have an influence on the σ-limits of the synchronous regime: the longest spatial-frequency mode, corresponding to the largest eigenvalue γ_1, and the shortest spatial-frequency mode, corresponding to the smallest eigenvalue γ_{N-1}. These both eigenvalues determine the width of synchronous σ-range and two types of desynchronizing bifurcations can
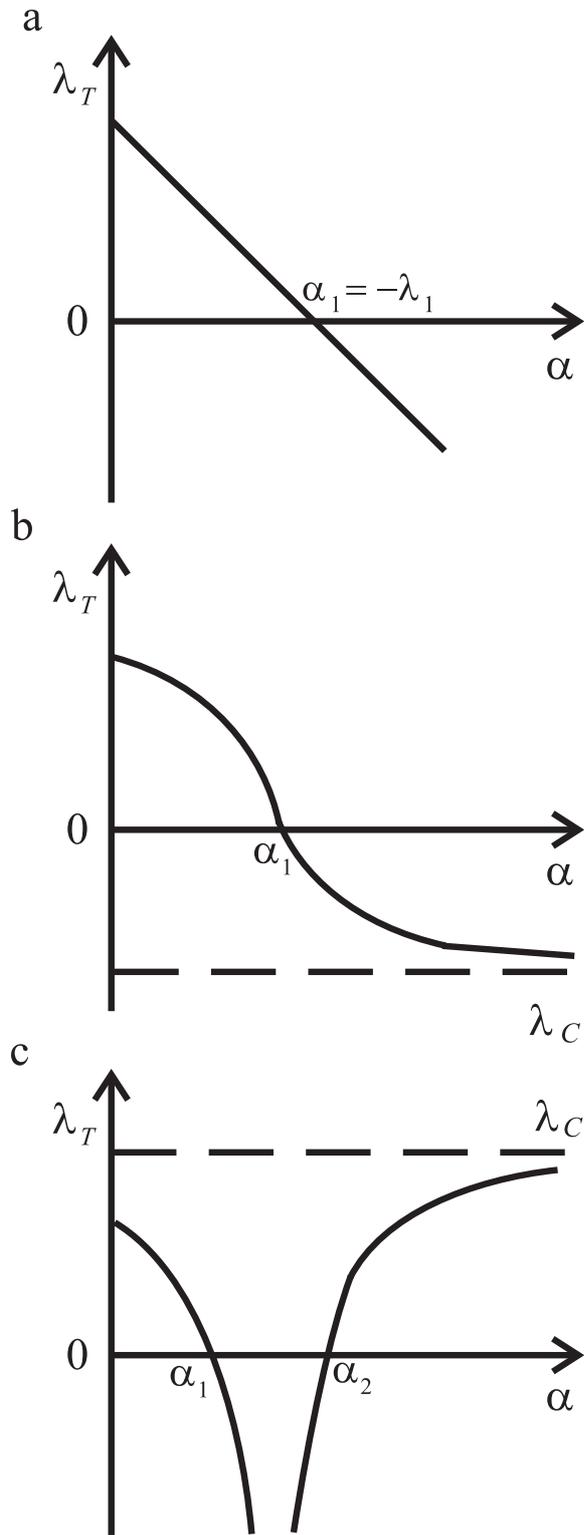
Fig. 1. Typical examples of MSF - $\lambda_T(\alpha)$ in the case of real coupling: (a, b) bottom-limited synchronous range (α_1, ∞), (c) double-limited synchronous interval (α_1, α_2).

occur when the synchronous state loses its stability [11]. Decreasing σ leads to a long wavelength bifurcation (LWB), because the longest wavelength mode γ_1 becomes unstable. On the other hand, the increase of the couplin strength causes the shortest wavelength mode γ_{N-1} to become unstable, thus a short wavelength bifurcation (SWB) takes place [11-13]. Another, characteristic feature of the coupled systems with double-limited synchronous interval is the array size limit, i.e. a maximum number of oscillators in an array which are able to synchronize. For the number of oscillators, which is larger then the size limit, the synchronous σ-interval does not exist. Such an interval exists if $\gamma_{N-1}/\gamma_1 < \alpha_2/\alpha_1$, where α_1 and α_2 are the boundaries of synchronous -α -interval (see Fig. 1c) [10-13]. If the synchronous range is only bottom-limited as it is depicted in Figs 1a and 1b, then the boundary (the smallest) value of σ, required for the appearance of synchronization, is determined only by the value of γ_1 and then desynchronizing LWB occurs with the decrease of σ. A type of single synchronous range appearing in the systems with PD coupl g depends on conditional Lyapunov exponents (CLEs) [4] of the remaining, uncoupled sub-block of node system. This property results from the asymptotic effect of the PD coupling [12-13]. An essence of this effect, depicted in Figs 1b and 1c, is that the largest TLE (MSF) tends asymptotically to the value of the largest CLE (λ_C) for strong coupling. Therefore, for negative λ_C the synchronous range is only bottom-limited (Fig. 1b) and for positive λ_C such a range is double-limited (Fig. 1c).

In numerical studies van der Pol's oscillator

$$\dot{x} = z \tag{8a}$$
$$\dot{z} = d(1 - x^2)z - x + cos(\Omega\tau), \tag{8b}$$

where d and Ω are constant, has been taken as an array node. Ω represents the frequency of the external excitation. The evolution of each oscillator coupled in 3-dimensional array is given by

$$\dot{x}_1 = z_1, \tag{9a}$$

$$\dot{z}_1 = d(1 - x_1^2)z_1 - x_1 + cos(\Omega\tau) + \sigma(x_2 - x_1), \tag{9b}$$

$$\dot{x}_2 = z_2, \tag{9c}$$

$$\dot{z}_2 = d(1 - x_2^2)z_2 - x_2 + cos(\Omega\tau) + \sigma(x_1 + x_3 - 2x_2), \tag{9d}$$

$$\dot{x}_3 = z_3, \tag{9e}$$

$$\dot{z}_3 = d(1 - x_3^2)z_2 - x_2 + cos(\Omega\tau) + \sigma(x_2 - x_3), \tag{9f}$$

where σ is a constant coupling coefficient and $i = 1, 2, 3$.

Fig. 2. The model of an open array of van der Pol's oscillators.

In the numerical analysis we assumed $d = 0.401$ and considered Ω and σ as control parameters. Eqs. (8) model, for example, a chain (the nearest-neighbor configuration of couplings) of 3 van der Pol's oscillators coupled in the open chain shown in Fig. 2. Such a connection of oscillators can be classified as the case of pure (diagonal components are equal to zero) ND coupling due to the form of output function

$$\mathbf{H} = \begin{bmatrix} 0 & 0 \\ 1 & 0 \end{bmatrix}. \tag{10}$$

The structure of the nearest-neighbor connections of array nodes is described by the following connectivity matrix

$$\mathbf{G} = \begin{bmatrix} -1 & 1 & 0 \\ 1 & -2 & 1 \\ 0 & 1 & -1 \end{bmatrix}. \tag{11}$$

Matrix $\mathbf{G}$ has the following eigenvalues $\gamma_0 = 0, \gamma_1 = -1, \gamma_2 = -3$. Since nonzero eigenvalues are not equal to each other one can expect the appearance of RSA. Substituting the analyzed system (Eqs (8) and (10)) in Eq. (6) we obtain the generic

variational equation for calculating the MSF, i.e., $\lambda_T(\alpha)$ in the form

$$\dot{\zeta} = \psi, \tag{12a}$$

$$\dot{\psi} = d(1 - x^2)\zeta - 2dx\psi\zeta - \psi + \alpha\psi. \tag{12b}$$

III. NUMERICAL AND EXPERIMENTAL RESULTS

Figure 3 presents the value of the synchronization error

$$e = \sum_{i=2}^{3} \sqrt{(x_1 - x_i)^2 + (z_1 - z_i)^2}, \tag{13}$$

versus the coupling coefficient σ and the frequency of external excitation Ω.
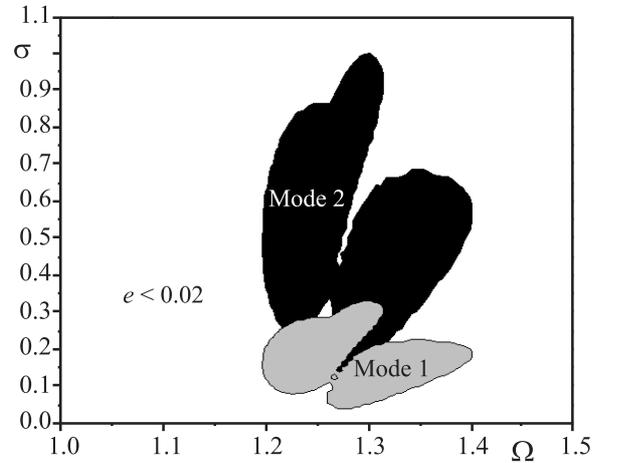
Fig. 3. The synchronization error $e = \sum_{i=2}^{3} \sqrt{(x_1 - x_i)^2 + (z_1 - z_i)^2}$ versus coupling coefficient σ and the frequency of external excitation Ω for Eqs. (9): $d = 0.401$.

In the white region $e < 0.02$ so we assumed that the systems are synchronized, grey and black regions denote desynchronization connected with the modes associated with eigenvalues γ_1 and γ_2 respectively. The calculations have been performed according to the idea of MSF for the probe of two oscillators [12-13]. One can expect RSA to appear for $\Omega \in (1.2, 1.5)$.

As an example consider $\Omega = 1.22$, i.e., in the absence of coupling each oscillator shows periodic behavior with the period equal to the period of excitation. In Fig. 4(a,b) we present the bifurcation diagrams of MSF versus the coupling coefficient σ. The diagram shown in Fig. 4(a) is based on the
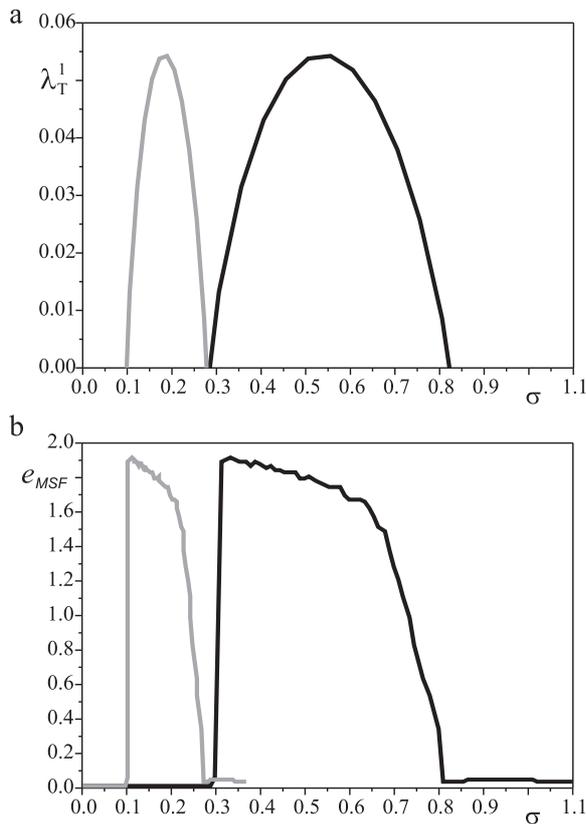
Fig. 4. Bifurcation diagrams of MSF versus coupling coefficient σ: $d = 0.401$, $\Omega = 1.22$; (a) diagram based on the transverse Lyapunov exponent λ_T^1, desynchronization intervals connected with eigenvalues γ_1 and γ_2 are shown in grey and black respectively, (b) diagram based on the synchronization error e_{MSF} calculated according to two oscillators probe.

transverse Lyapunov exponent λ_T^1 (desynchronization intervals connected with eigenvalues γ_1 and γ_2 are shown in grey and black respectively), while the one in Fig. 4(b) on the synchronization error e_{MSF} calculated according to two oscillators probe [12,13]. In both diagrams the ragged synchronizability is visible as the 'windows' of synchronization and desynchronization can be observed, before the final synchronous state is achieved due to the increase of the coupling strength at $\sigma = 0.8$.

To confirm the existence of RSA in the real systems we have performed an experiment in which van der Pol's oscillator has been implemented as an electronic circuit [17]. We have considered dynamics of three circuits coupled in the way described in Sec. 3. An example of typical experimental results is shown in Fig. 5, were we plot the synchronization error e versus σ. These results have been obtained

for the same parameter values as the numerical results of Fig. 4(a,b).
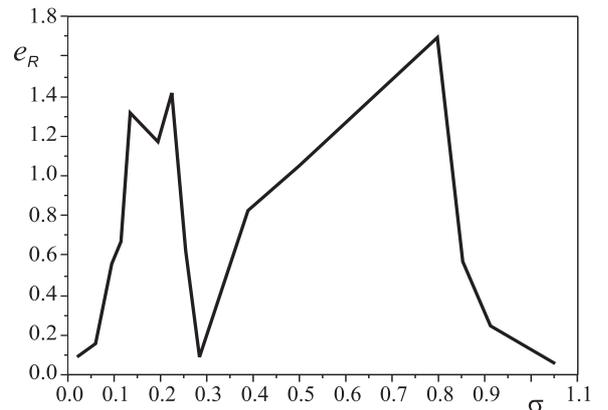
Fig. 5. Experimental synchronization error e versus σ: $d = 0.401$, $\Omega = 1.22$.

It should be mentioned here that in the experiments it is impossible to avoid parameter mismatches so the complete synchronization is replaced by the imperfect complete synchronization in which synchronization error is sufficiently small but not equal to zero. One can see a good agreement in both results. The details of this experiment will be reported elsewhere [18].

In considered network one can observe the phenomenon of clustering [19,20]. Such behaviour corresponding to existence one or more groups of synchronized oscillators although the whole network is in the desynchronized state. In our case we can obviously observe only (2,1) cluster, i.e, two nodes have common behaviour and one node is independent. We defined the synchronization errors between first and second ($e_{1-2} = \sqrt{(x_1 - x_2)^2 + (z_1 - z_2)^2}$) and first and third ($e_{1-3} = \sqrt{(x_1 - x_3)^2 + (z_1 - z_3)^2}$) oscillator. In Figure 6 we present results of numerical calculation of synchronization error e_{1-2} (black line) and e_{1-3} (grey line).

As it easy to see in range $\sigma = (0.1, 0.27)$ one can observed a cluster between fist and third oscillator, while second system is in the desynchronized state with them. This phenomenon is confirmed by calculation of eigenvectors [21] of connectivity matrix $\mathbf{G}$. The synchroniation in range $\sigma = (0.1, 0.27)$ is governed by eigenvalue $\gamma_2 = -3$ with corresponding eigenvector $v_2 = [1, -2, 1]$. This values of v_2
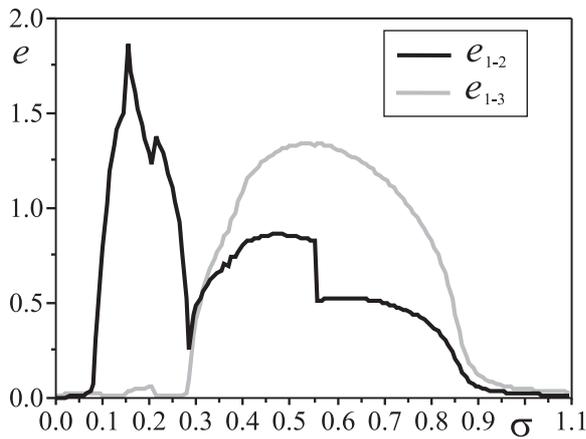
Fig. 6. Experimental synchronization error e versus σ: $d = 0.401$, $\Omega = 1.22$.

leads to existence of cluster shown in Figure 6.

IV. CONCLUSIONS

To summarize, we have confirmed and explained the phenomenon of the ragged synchronizability (RSA)in the networks of van der Pol's oscillators with ND coupling between the nodes. Its occurrence is independent of the motion character (periodic or chaotic) of an isolated node system. We have shown the mechanism responsible for the appearance or disappearance of the windows of synchronizability is the same as the previously studied network of Duffing oscillators [16]. It seems that the phomenonon of RSA is common for the systems with non-diagonal coupling and not sensitive for the small parameter mismatch, i.e., can be observed in real experimental systems.

REFERENCES

[1] V. S. Afraimovich, N. N. Verichev, and M. Rabinovich, Izv. Vusov. Radiofizika 28(9) (1985)1050.
[2] Blekhman I., *Synchronization in Science and Technology* (ASME Press, New York, 1988);
[3] L.M. Pecora, T.L. Carroll, Phys. Rev. Lett. 64 (1990) 821.
[4] S. Boccaletti, J.Kurths, D. Osipov, D.L. Valladares, and C.S.Zhou, Physics Reports 366 (2002) 1.
[5] H. Fujisaka and T. Yamada, Prog. Theor. Phys. 69 (1983) 32.
[6] T. Yamada and H. Fujisaka, Prog. Theor. Phys. 70 (1983) 1240.
[7] A. Pikovsky, Zeitschrift Phys. B 55 (1984) 149.
[8] A. Stefaski, J. Wojewoda, T. Kapitaniak, S. Yanchuk S., Phys. Rev. E 70, 026217 (2004).
[9] S. Dmitriev, M. Shirokov and S. O. Starkov, IEEE Trans. Circuits Syst. I. Fund. Th. Appl. 44(10) (1997) 918.
[10] L. M. Pecora and T. L. Carroll, Phys. Rev. Lett. 80(10) (1998) 2109.
[11] L. M. Pecora, Phys. Rev. E 58(1) (1998) 347.
[12] L. M. Pecora and T. L. Carroll, G. Johnson, D. Mar, K. Fink, Int. J. Bifurcation Chaos 10(2) (2000) 273.
[13] K. Fink, G. Johnson, T. L. Carroll, D. Mar, and L. M. Pecora, Phys. Rev. E 61 (2000) 5080.
[14] M. Barahona and L. M. Pecora, Phys. Rev. Lett. 89 (2002) 054101.
[15] T. Nishikawa, A. E. Motter, Y.-C. Lai, and F. C. Hoppensteadt, Phys. Rev. Lett. 91(1) (2003) 014101.
[16] A. Stefanski, P. Perlikowski and T. Kapitaniak, Phys. Rev. E 58(1) (2007) 347.
[17] B. Nana, P. Woafo, Phys. Rev. E, 74, (2006), 046213.
[18] P. Perlikowski, A. Stefanski and T. Kapitaniak, in preparation.
[19] Belykh V. N., Belykh I. V., Mosekilde E.: Cluster synchronization modes in an ensemble of coupled chaotic oscillators. Phys. Rev. E, 63(3):036216, 2001.
[20] Kaneko K.: Clustering, coding, switching, hierarchical ordering, and control in network of chaotic elements. Physica D, 41:137172, 1990.
[21] Yanchuk S., Maistrenko Y., Mosekilde E.: Partial synchronization and clustering in a system of diffusively coupled chaotic oscillators. Math. Comp. Simul. 54, (2000), 491.